Measurements of the parallel wavenumber of lower hybrid waves in the scrape-off layer of a high-density tokamak

Citation: Baek, S. G. et al. "Measurements of the Parallel Wavenumber of Lower Hybrid Waves in the Scrape-Off Layer of a High-Density Tokamak." Physics of Plasmas 23, 5 (May 2016): 050701

As Published: http://dx.doi.org/10.1063/1.4948555

Publisher: American Institute of Physics (AIP)

Persistent URL: http://hdl.handle.net/1721.1/111180

Version: Author's final manuscript: final author's manuscript post peer review, without publisher's formatting or copy editing

PSFC/JA-16-58

Measurements of the parallel wavenumber of lower hybrid waves in the scrape-off layer of a high-density tokamak

S. G. Baek, G. M. Wallace, T. Shinya*, R. R. Parker,
S. Shiraiwa, P. T. Bonoli, D. Brunner, I. Faust, B. L. LaBombard,
Y. Takase*, S. Wukitch

*University of Tokyo, Kashiwa, Japan

April, 2016

Plasma Science and Fusion Center
Massachusetts Institute of Technology
Cambridge MA 02139 USA

This work was conducted on the Alcator C-Mod tokamak, a DoE Office of Science user facility, and supported by U.S. DoE Cooperative Agreement No. DEFC02-99ER54512 and Japan/U.S. Cooperation in Fusion Research and Development. The authors would like to thank the Alcator C-Mod team for supporting this experiment.

Measurements of the parallel wavenumber of lower hybrid waves in the scrape-off layer of a high-density tokamak

S. G. Baek, G. M. Wallace, T. Shinya*, R. R. Parker, S. Shiraiwa, P. T. Bonoli, D. Brunner, I. Faust, B. L. LaBombard, Y. Takase*, and S. Wukitch

MIT Plasma Science and Fusion Center, Cambridge, MA, USA
*University of Tokyo, Kashiwa, Japan

In lower hybrid current drive experiments on tokamaks, the parallel wavenumber of lower hybrid waves is an important physics parameter that governs the wave propagation and absorption physics. However, this parameter has not been experimentally well-characterized in present-day high density tokamaks, despite the advances in the wave physics modeling. In this paper, we present the first measurement of the dominant parallel wavenumber of lower hybrid waves in the scrape-off layer (SOL) of the Alcator C-Mod tokamak with an array of magnetic loop probes. The electric field strength measured with the probe in typical C-Mod plasmas is about one-fifth of that of the electric field at the mouth of the grill antenna. The amplitude and phase responses of the measured signals on the applied power spectrum are consistent with the expected wave energy propagation. At higher density, the observed $k_{\|}$ increases for the fixed launched $k_{\|}$, and the wave amplitude decreases rapidly. This decrease is correlated with the loss of LHCD efficiency at high density, suggesting the presence of loss mechanisms. Evidence of the spectral broadening mechanisms is observed in the frequency spectra. However, no clear modifications in the dominant $k_{\|}$ are observed in the spectrally broadened wave components, as compared to the measured k|| at the applied frequency. It could be due to (1) the probe being in the SOL and (2) the limited $k_{\|}$ resolution of the diagnostic. Future experiments are planned to investigate the roles of the observed spectral broadening mechanisms on the LH density limit problem in the strong single pass damping regime.

On tokamaks, lower hybrid (LH) waves are used to drive toroidal plasma current [1], and their application on reactor-relevant tokamaks as a current drive actuator is an active research area [2-6]. On the Alcator C-Mod tokamak [7], the lower hybrid current drive (LHCD) system [8] at f_0 = 4.6 GHz operates at ITER- and reactor- relevant conditions with relatively low temperatures ($T_{e0} \approx 2$ keV in L-mode plasmas, as opposed to 15 keV in ITER). As a result, the LH waves launched at the outer mid-plane are weakly absorbed on a single-pass, and the waves may undergo multiple parasitic edge loss mechanisms [9, 10, 11, 12, 13] at the plasma edge before being absorbed via electron Landau damping (ELD) in the plasma core. In particular, the wave-power reaching the high field side (HFS) of the C-Mod tokamak was found to decrease as density increases above $\bar{n}_e = 1.0 \times 10^{20}$ m^{-3} [14]. Further, a recent ray-tracing modeling study [15] indicates that

collisional absorption could explain the observed anomalous decrease in hard X-ray count rates (thus fast electron populations) in high density plasmas, consistent with the experimental observation of the enhanced ionization rate in the active divertor region with the applied LH power [2]. In the single-pass damping regime, *e.g.* in ITER, these parasitic loss mechanisms are expected to be mitigated because the waves will be absorbed strongly on the first pass via ELD, which will also be beneficial in driving off-axis current. However, the waves will still need to propagate across the edge/scrape-off-layer (SOL) plasma from the launcher to the plasma, which is about 12 cm in ITER [16] as opposed to 2 cm in C-Mod, where waves could be susceptible to various loss mechanisms depending on the details of plasma conditions. Thus, the wave propagation on the first pass needs to be fully characterized to predict LHCD performance in future tokamaks.

Our goal in this paper is to develop a diagnostic to characterize wave propagation, in particular the parallel refractive index ($n_{||} \equiv ck_{||}/\omega_0$) of LH waves. Here, c is the speed of light, ω_0 is the angular frequency of the wave, and $k_{||} \equiv \vec{k} \cdot \vec{B}/|B|$ is the parallel wave-number along the background magnetic field. The $n_{||}$ is an important physics parameter determining wave propagation and absorption — not only Landau absorption but also additional parasitic absorption mechanisms, such as collisional damping [17] and parametric instabilities [18]. The $n_{||}$ quantification is also important from a viewpoint of modeling the LH physics as several recent modeling works propose the importance of the ponderomotive force [10,19], and the redistribution of the power spectrum on the first pass before crossing the separatrix [4, 20, 21].

In this paper, we report our first proof-of-principle measurements of the parallel wavenumber of lower hybrid waves in the SOL of the C-Mod tokamak near the launcher using a magnetic probe array. As compared to the use of a single probe that is often placed outside the vacuum vessel, this approach allows us to examine the $n_{||}$ and coherence at a known wave polarization near the plasma, in addition to the frequency spectrum of the wave. In the remainder of this paper, we first describe the experimental setup developed on C-Mod. Then we discuss the phase and amplitude responses of the measured signals as a function of the applied spectrum at the launcher. Finally, we

investigate the dependences of the measured amplitude and phase on density, and present evidence of spectral broadening mechanisms in high density plasmas.

As shown in Figure 1(a), the probe array consists of the two rows of three magnetic probes. The probes in the top row are sensitive to the magnetic signals that oscillate in the poloidal direction (or y-direction), and the probes in the bottom row are sensitive to the magnetic signals that oscillate along the background magnetic field. The diameter of the loop probe is 1.2 mm. A slit covered with a ceramic plate allows the wave to propagate toward the loop probe while preventing direct electrostatic coupling [22]. In each row, the probes are separated by Δz = 6.5 mm along the background magnetic field direction, which allows us to discern the $n_{||} = (c\Delta\varphi/\Delta z)/\omega_0$ up to ~5.5. With the three magnetic probes in a row, the dominant $n_{||}$ can be determined from the least square fitting of the relative phases found from the cross spectral analysis. In this paper, we focus on the signals measured with the probes in the top row as they are the dominant magnetic field component of the slow LH wave. The probe array is located 20 cm below the midplane, and about 108 degrees toroidally away from the LH grill launcher, and it is magnetically mapped to the launcher for a wide range of plasma currents (Figure 1(b)). The radial location of the probe head is about 2 cm behind the separatrix.

The signals measured at 4.6 GHz are directly digitized by frequency down-converting to 25 MHz with the use of two frequency mixing stages [23]. A high-speed, high-resolution digitizer is triggered to sample 8192 data points at a rate of 100 mega-samples/sec for every 10 milliseconds. In the analysis, the data sampled in each trigger event are divided into 6 segments to perform a cross spectral analysis to deduce (1) the auto-power, (2) the dominant $n_{||}$, and (3) the magnitude squared coherence (γ^2) spectrograms as functions of time and frequency. Care was taken to calibrate out the relative phase difference among the channels by using a slotted waveguide and a network analyzer.

The LH waves launched from the grill antenna are expected to propagate toward the probe head on the first pass along and nearly parallel to the background magnetic field lines due to their electrostatic nature [24]. The power spectrum launched with the grill antenna has a finite width in the $n_{||}$ space due to a finite number of radiating elements along the toroidal direction. Based on the absolute power calibration with a slotted

waveguide, we find that the parallel wave electric-field is measured to be $|E_{\parallel}| \approx 30$ kV/m with typical experimental parameters ($\bar{n}_e = 1.1 \times 10^{20}$ m^{-3}, $I_p = 1.1$ MA, $P_{LH} = 300$ kW, and the peak $n_{||}$ in the launched power spectrum = 1.6), assuming that $|E_x|/|E_{\parallel}| = \sqrt{P/S} \approx \sqrt{\omega_{pe}/\omega_0} = 3.7$ with $n_e = 0.5 \times 10^{20}$ m^{-3}, and $|B_y|/|E_x| \approx S/(n_{\parallel}c) \approx 1/(n_{\parallel}c)$ from the Maxwell-Ampere equation neglecting the cross-coupling term in the cold plasma dielectric tensor (*i.e.* $D = 0$) with D, P and S defined following Stix's notation [25]. As compared to $|E_{\parallel}| \approx 140$ kV/m in the grill antenna that is found by considering the wave impedance [26] and the power flow within a single grill antenna, this value appears to be reasonable as the probes are not expected to directly intercept the resonance cone, as indicated by a ray-tracing model shown later. When the background magnetic field and plasma current is reversed, the LHCD system is configured such that the waves propagate in the opposite toroidal direction. In that case, as compared to the measurements above, (1) the measured peak power is lower by two orders of magnitude, (2) the standard deviation of the measured phase is about ten times higher, and (3) the measured squared coherence is lower by 60%, all of which strongly suggest that the probes detect the coherent wave-fields directly leaving the launcher in the standard field configuration.

A detailed ray-tracing study using GENRAY [27] shows that the wave-fields with the low $n_{||}$ end of the launched power spectrum will be dominantly measured with the probe. Figure 2 shows the poloidal projection of the ray propagation paths from the launcher to the toroidal location where the probe head is located at two different initial launched $n_{||}$ values. To estimate the poloidal spreading, the rays at four different poloidal locations are initiated to simulate the four rows of the grill antenna. Assumed parameters in the simulation are $\bar{n}_e = 1.2 \times 10^{20}$ m^{-3}, and $I_p = 1.1$ MA. In the SOL, both density and temperature profiles are assumed to exponentially decay across the flux surface. It is important to note that the details in the ray trajectory will be dependent on plasma density, magnetic field, and plasma current. In Figure 2(a), the $n_{||}$ generally down-shifts on the first pass due to the angular dependence of the evolution in the poloidal mode number [28]. Figure 2(b) shows that, when the initial $n_{||}$ is low enough, the rays could propagate along the LCFS in front of near the probe head. The ratio of the perpendicular to parallel

group velocity of a ray increases with $n_{\parallel}$ according to the equation: $\frac{v_{g\perp}}{v_{g\parallel}} \approx \frac{\omega_0}{\omega_{pe}}\sqrt{1-\frac{1}{n_{\parallel}^2}}$. It is also seen that if $n_{\parallel}$ does not meet the accessibility condition, the ray is trapped at the boundary between the mode-conversion and cut-off layers.

This ray-tracing simulation is consistent with a controlled experiment in which the applied $n_{\parallel}$ spectrum is varied at the fixed plasma parameters ($\bar{n}_e = 1.1 \times 10^{20}$ m^{-3}, I_p = 1.1 MA). For example, Figure 3(a) shows two power spectra launched with the peak $n_{\parallel}$ at 1.6 and 1.9. Figure 3(b) shows that the dominant $n_{\parallel}$ measured at 4.6 GHz nearly remains at a constant value ($n_{\parallel}$ = 1.6 in this particular case), independent of the change in the applied spectrum. Thus, the probe system detects the same spectral component of the wave-field in moderate-density plasmas at the fixed plasma parameters. As shown in Figure 3(c), the measured wave power decreases exponentially with the increase in the applied peak $n_{\parallel}$. This is consistent with the decrease in the spectral power content at $n_{\parallel}$ = 1.6 in the applied spectrum as the applied peak $n_{\parallel}$ increases from 1.6 to 2.4. In all cases, γ^2 remains high above 90%.

Figure 4(a) shows the dominant $n_{\parallel}$ measured both at 4.6 GHz and 4.57 GHz as a function of plasma density at three different plasma currents. The signals at 4.57 GHz are a result of the onset of ion cyclotron parametric decay instabilities, which may be linked to the observed LHCD density limit problem [14]. Given the frequency separation, this instability is expected to occur at the LFS edge on the first pass from the launcher to the plasma. As shown in Figure 4(a), the dominant $n_{\parallel}$ measured at 4.6 GHz is found to increase as density increases. Regardless of plasma current, density is found to be a strong parameter in determining the measured $n_{\parallel}$. The peak in the applied $n_{\parallel}$ spectrum is fixed at 1.6. As density increases, this peak n|| component will undergo multiple reflections between the mode conversion and reflection layers because of the accessibility condition: $n_{acc} \approx 5\text{x}10^{19}$ m^{-3} at the low-field-side (LFS) edge (4.1 T). If it is a fast wave at the probe location, it may not be detected with the probe of interest. Further, this increase in the measured $n_{\parallel}$ is qualitatively consistent with the radially outward-shift of the resonance cone as the waves will have a limited radial penetration with the increase in plasma density ($\frac{v_{g\perp}}{v_{g\parallel}} \approx \frac{\omega_0}{\omega_{pe}}\sqrt{1-\frac{1}{n_{\parallel}^2}}$).

Figure 4(a) also shows that the dominant $n_{||}$ measured at 4.57 GHz tracks that of the main signal at 4.6 GHz. A previous growth rate calculation shows a higher growth rate at a higher $n_{||}$ of the sideband LH wave [14]. Further, in the previous laser scattering experiment on Alcator C, the ion cyclotron sideband LH wave are measured to have high $n_{||}$ components in the plasma core [29, 30]. Thus, it is possible that the probes are not placed at the region where instabilities occur near the launcher, and those high $n_{||}$ components could have radially propagated inward, or away from the probe head by the time they pass by the toroidal location where the probe head is located. Note that one caveat in the experimental result presented is that unless the averaged $n_{||}$ is significantly changed, it would not be possible to identify such a shift in $n_{||}$ in the present study because only the dominant $n_{||}$ is deduced in the analysis.

Figure 4(b) shows that the peak power measured both at 4.6 GHz and 4.57 GHz. The peak power measured at 4.6 GHz decreases by two orders of magnitude as density increases. It is interesting to note that the fall-off rates in the measured wave power is dependent on the magnitude of plasma current, which correlates with a weaker fall-off rate of the hard X-ray emission at higher current [14]. For example, the wave power measured at $\bar{n}_e = 1.1 \times 10^{20}$ m^{-3} in the I_p =0.8 MA case is higher by an order of magnitude than that in the I_p = 0.6 MA case. In low current plasmas, parasitic loss mechanisms are expected to aggravate as the SOL width broadens [31]. Since not much power is deposited in the core at high density [2], this power decrease in the LFS SOL may hint at the presence of SOL/edge power loss mechanisms. Note that the measured wave component at high density with $n_{||} \approx 2$ is accessible to plasma core.

Figure 4(b) also shows that the onset of the sideband LH wave at 4.57 GHz is dependent on plasma current. With the onset, the wave power at the source frequency starts to decrease, suggesting that the wave power could have partly been depleted due to the observed instability. However, the sideband power remains to be lower by an order of magnitude, and starts to decrease at high density concurrently with the decrease in the wave power at 4.6 GHz. It is possible that both waves suffer from collisions. This observation also motivates to investigate in future studies whether the parametrically excited sideband LH wave with high $n_{||}$ components could generate enough fast electrons at the plasma edge that could act as a target for the relatively low n|| wave at the source

frequency, which could subsequently limit the wave penetration. As shown in Figure 4(c), the magnitude squared coherence at 4.6 GHz decreases below 90% above the density at which the sideband power is peaked. Taking γ^2 as a measure of the phase consistency, this may indicate the effects of wave scattering or a longer wave propagation path.

Figure 5 shows the measured decrease in wave power as a function of density (or the measured $n_{||}$ based on the observed dependence of the measured $n_{||}$ on density in Figure 4) at two different applied peak $n_{||}$: 1.6 and 2.0. Note that in the peak $n_{||}$ = 2.0 case, the measured n|| exhibits a similar density dependence to the $n_{||}$ = 1.6 case (Figure 3). The measurements are compared to the change in the spectral power components at the measured $n_{||}$ in the launched spectra, indicated by dotted lines. In the $n_{||}$ = 1.6 case, the measured wave power scales to the decrease in the spectral power deduced from the applied spectrum as a function of the measured $n_{||}$. On the other hand, in the n|| = 2.0 case in which the launched spectrum is accessible, the measured power decreases rapidly at high density, whereas the spectral power found from the antenna spectrum increases by an order of magnitude as $n_{||} \rightarrow 2$. Thus it proves to be difficult to ascertain that the observed wave-field at high density is solely due to the wave-field leaving the launcher. To identify which wave components are measured, a more detailed modeling study will be necessary, in particular at high densities ($>1.2 \times 10^{20}$ m^{-3}) where the measured power is found to be insensitive to the launched power spectrum.

In summary, the dominant $n_{||}$ of the LH waves has been successfully measured in the SOL of the Alcator C-Mod tokamak with an array of magnetic loop probes. Given that the LH waves will be strongly absorbed by the plasma in future reactors, it is important to study the wave propagation study on the first pass in the SOL. At moderate densities, the observed power and $n_{||}$ responses on the applied power spectrum are consistent with a ray-tracing picture, suggesting that the probes dominantly measure the wavefield leaving the launcher. However, at high density, coherence decreases below 90%, and the measured wave power rapidly decreases, which may indicate the roles of the accessibility condition and/or parasitic loss mechanisms, which are sensitive to edge plasma conditions, as indicated by the observed plasma current dependence. While the onset of ion cyclotron parametric instabilities that is expected to occur on the first pass is observed, no strong modification in the dominant $n_{||}$ is observed in those wave components, which

is likely due to (1) the limited $n_{||}$ resolution in the diagnostic and/or (2) the measurement location being in the SOL. Thus, in this experiment, no clear causality is identified between the observed ion cyclotron parametric instabilities and the anomalous loss of LHCD efficiency. Roles of these spectral broadening mechanisms on the loss of efficiency will be further clarified in future experimental studies in which the launched LH wave will be strongly single pass absorbed. In addition, as it is critical to establish that the probes can directly detect the wavefield launched from the antenna even at high density, a new probe array will be placed closer to the LH launcher (36° toroidally vs. 108°), so that the probes could be more sensitive to the primary resonance cone. It is also planned to increase the number of probes to perform a Fourier analysis of the measured signal in the $n_{||}$ space.

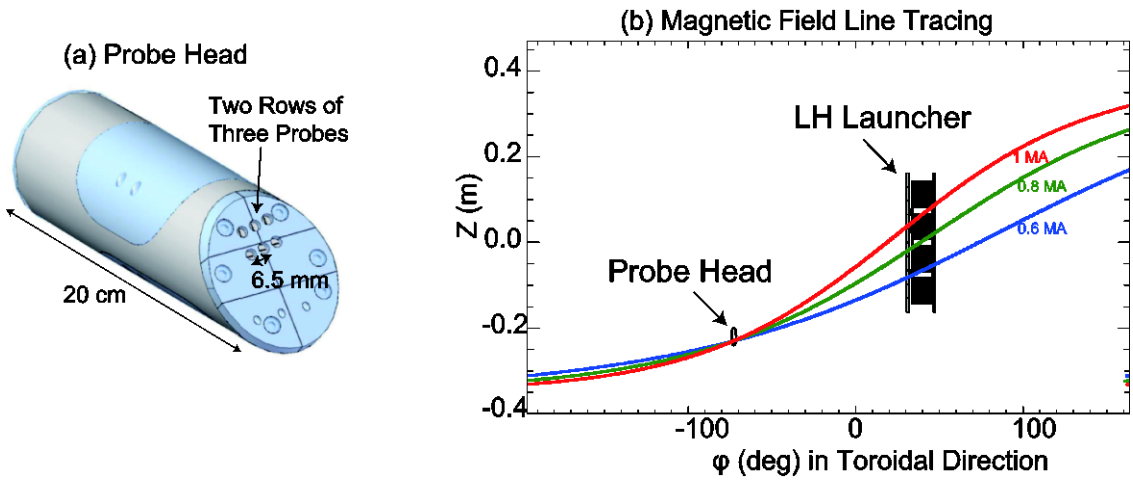

Figure 1: (a) CAD drawing of a probe head that holds two rows of three magnetic loop probes. (b) Magnetic field-line tracing starting from the probe array location at three different plasma currents (0.6, 0.8, and 1.0 MA).

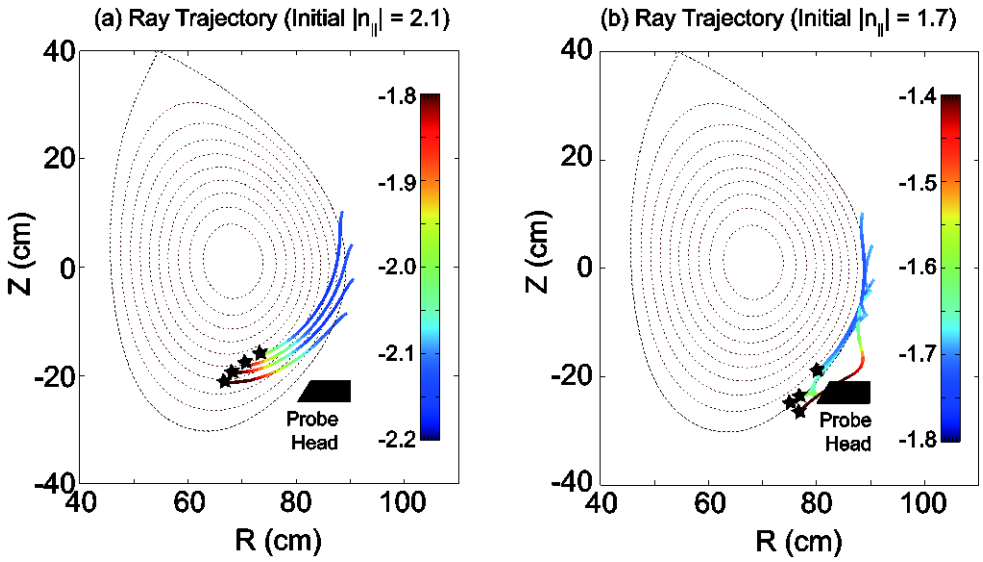

Figure 2: The poloidal projection of the LH ray trajectories from the grill antenna to the probe head location with the initial ray $n_{||}$ at (a) 2.1 and (b) 1.7. The negative $n_{||}$ in the color bar indicates that the rays are propagating in the opposite direction to the plasma current. The black stars show that the rays are terminated at the toroidal location where the probe is placed. Assumed parameters are: $\bar{n}_e \approx 1.2 \times 10^{20}$ m^{-3}, I_p = 1.1 MA.

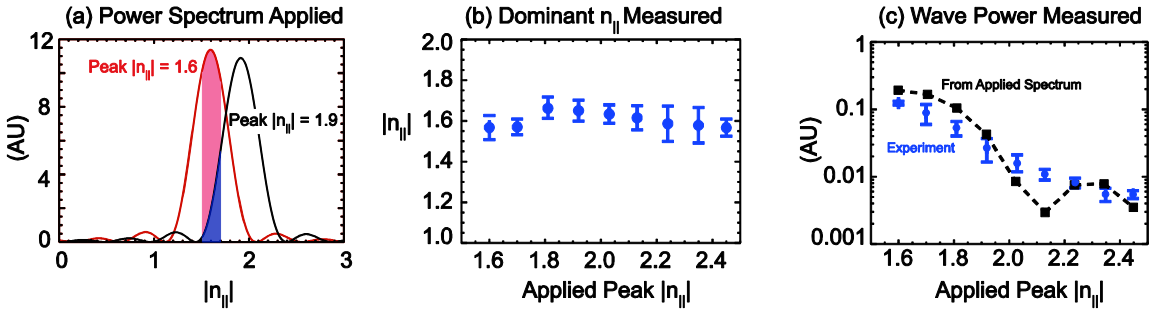

Figure 3: (a) An example of the applied power spectra at the grill antenna with the peak $n_{||}$ at 1.6 and 1.9. The corresponding spectral power contents at $n_{||}$ = 1.6 ± 0.1 are marked with the red and blue colors, respectively. (b) The dominant $n_{||}$ is measured as a function of the applied peak $n_{||}$. (c) The peak wave power is measured as a function of the applied peak $n_{||}$. The dotted line refers to the spectral power content at $n_{||}$ = 1.6 ± 0.1 in the applied power spectrum with different $n_{||}$ peaks. Experimental parameters are $\bar{n}_e = 1.1 \times 10^{20}$ m^{-3}, I_p = 1.1 MA, P_{LH} = 300 kW, and the launched peak $n_{||}$ = 1.6.

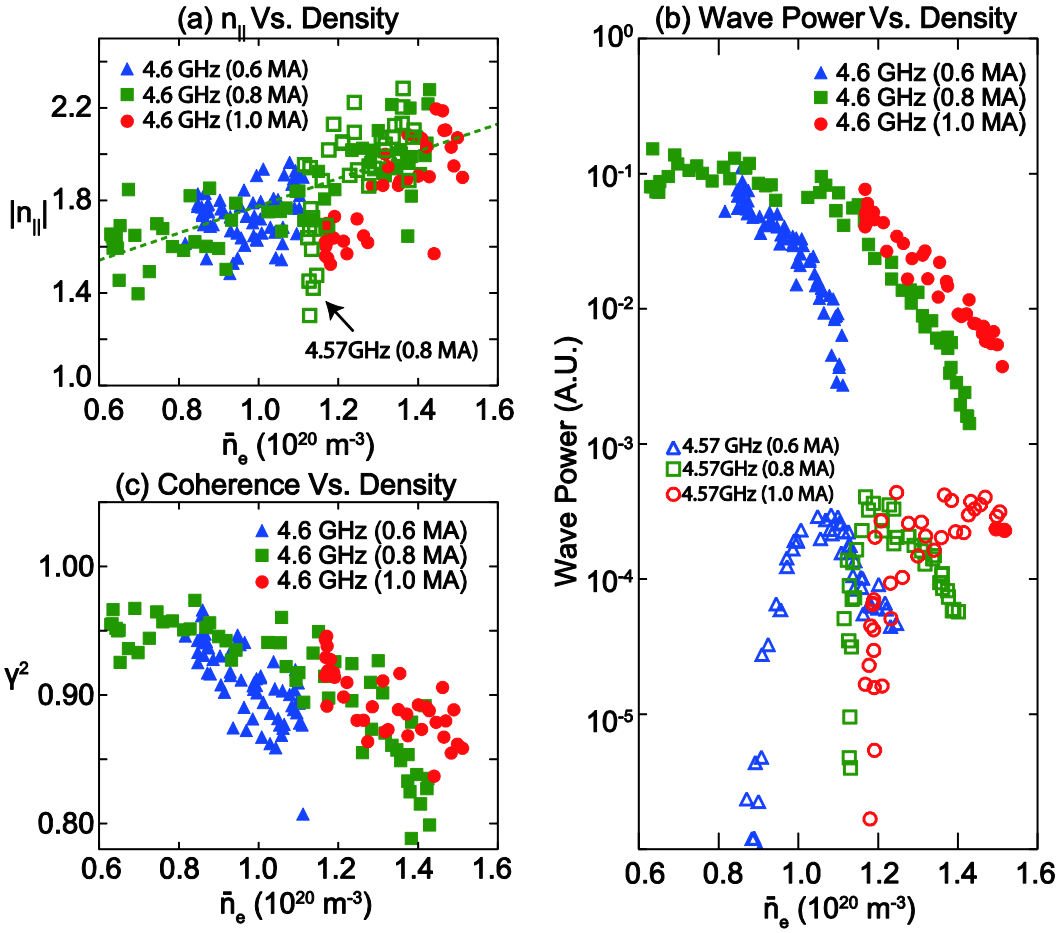

Figure 4: (a) the dominant $n_{||}$, (b) the wave power, and (c) the magnitude squared coherence measured as a function of the line-averaged density ($\bar{n}_e$) at three different plasma currents (▲: 0.6 MA, ■: 0.8 MA, and ●: 1 MA). In (a) and (b), the filled symbols represent the measurements at 4.6 GHz and unfilled ones at 4.57 GHz. In (a), the dotted line indicates the least square fitting of the dominant $n_{||}$ measured at 4.6 GHz as a function of density in the Ip = 0.8 MA case.

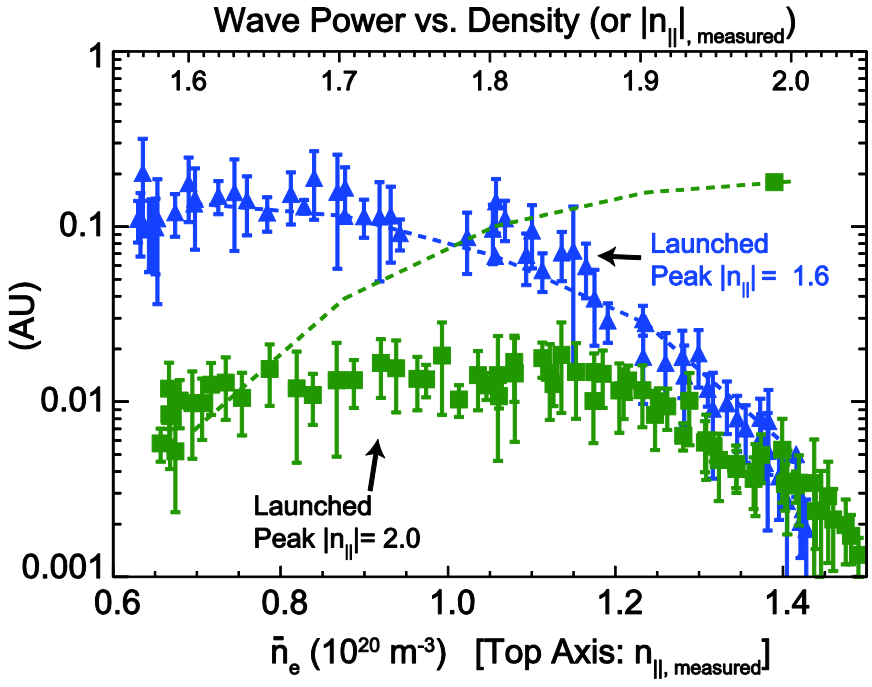

Figure 5: The peak power measured at 4.6 GHz as a function of $\bar{n}_e$ (or $n_{||,\,measured}$) at two different applied $n_{||}$ peaks: $n_{||,peak}$ = 1.6 (▲) and $n_{||,peak}$ = 2.0 (■). Plasma parameters are identical to the 0.8 MA case in Figure 4. The dotted lines denote the spectral power content found from the applied antenna spectrum (*e.g.*, Figure 3(a)) by identifying the fractional spectral power content in the range ($n_{||,measured}$ – 0.1, $n_{||,measured}$ + 0.1) in the applied antenna spectrum.

This work was conducted on the Alcator C-Mod tokamak, a DoE Office of Science user facility, and supported by US DoE Cooperative agreement DE-FC02-99ER54512 and Japan/U. S. Cooperation in Fusion Research and Development. The authors would like to thank the Alcator C-Mod team for supporting this experiment.

[1] N. J. Fisch and A. H. Boozer, *Phys. Rev. Lett.* **45**, 720 (1980)

[2] I. C. Faust, 57th Annual meeting of the APS Division of Plasma Physics 60, BAPS.2015.DPP.CP12.22 (2015), http://meetings.aps.org/link/BAPS.2015.DPP.VI2.3

[3] R. Cesario, L. Amicucci, A. Cardinali, C. Castaldo, M. Marinucci, F. Napoli, F. Paoletti, D. De Arcangelis, M. Ferrari, A. Galli, G. Gallo, E. Pullara, G. Schettini and A.A. Tuccillo, Nucl . Fusion 54, 043002 (2014)

[4] J. Decker, Y. Peysson, J.-F. Artaud, E. Nilsson, A. Ekedahl, M. Goniche, J. Hillairet, and D. Mazon, Phys. Plasmas 21, 092504 (2014)

[5] B.J. Ding, Y.C. Li, L. Zhang, M.H. Li, W. Wei, E.H. Kong, M. Wang, H.D. Xu, S.L. Wang, G.S. Xu, L.M. Zhao, H.C. Hu, H. Jia, M. Cheng, Y. Yang, L. Liu, H.L. Zhao, Y. Peysson, J. Decker, M. Goniche, L. Amicucci, R. Cesario, A.A. Tuccillo, S.G. Baek, R. Parker, P.T. Bonoli, F. Paoletti, C. Yang, J.F. Shan, F.K. Liu, Y.P. Zhao, X.Z. Gong, L.Q. Hu, X. Gao, B.N. Wan, J.G. Li and the EAST team, Nucl. Fusion 55, 093030 (2015)

[6] M. Goniche, V. Basiuk, J. Decker, P.K. Sharma, G. Antar, G. Berger-By, F. Clairet, L. Delpech, A. Ekedahl, J. Gunn, J. Hillairet, X. Litaudon, D. Mazon, E. Nilsson,T. Oosako, Y. Peysson, M. Preynas, M. Prou and J.L. Ségui, Nucl. Fusion 53, 03310 (2013)

[7] I. H. Hutchinson, R. Boivin, F. Bombarda, P. Bonoli, S. Fairfax, C. Fiore, J. Goetz, S. Golovato, R. Granetz, M. Greenwald, S. Horne, A. Hubbard, J. Irby, B. LaBombard, B. Lipschultz, E. Marmar, G. McCracken, M. Porkolab, J. Rice, J. Snipes, Y. Takase, J. Terry, S. Wolfe, C. Christensen, D. Garnier, M. Graf, T. Hsu, T. Luke, M. May, A. Niemczewski, G. Tinios, J. Schachter, and J. Urbahn, Phys. Plasmas 1, 1511 (1994)

[8] P. T. Bonoli, R. Parker, S. J. Wukitch, Y. Lin, M. Porkolab, J. C. Wright, E. Edlund, T. Graves, L. Lin, J. Liptac, A. Parisot, A. E. Schmidt, V. Tang, W. Beck, R. Childs, M. Grimes, D. Gwinn, D. Johnson, J. Irby, A. Kanojia, P. Koert, S. Marazita, E. Marmar, D. Terry, R. Vieira, G. Wallace, J. Zaks, S. Bernabei, C. Brunkhorse, R. Ellis, E. Fredd, N. Greenough, J. Hosea, C. C. Kung, G. D. Loesser, J. Rushinski, G. Schilling, C. K. Phillips, J. R. Wilson, R. W. Harvey, C. L. Fiore, R. Granetz, M. Greenwald, A. E. Hubbard, I. H. Hutchinson, B. LaBombard, B. Lipschultz, J. Rice, J. A. Snipes, J. Terry, S. M. Wolfe, and Alcator C-Mod Team, Fusion Sci. Technol. 51, 401 (2007)

[9] G. Wallace, R. Parker, P. Bonoli, A. Hubbard, J. Hughes, B. LaBombard, O. Meneghini, A. Schmidt, S. Shiraiwa, D. Whyte, J. Wright, S. Wukitch, R. Harvey, A. Smirnov, and J. R. Wilson, Phys. Plasmas 17, 082508 (2010)

[10] O. Meneghini, Ph.D. dissertation, MIT, 2012

[11] S. Baek, R. Parker, S. Shiraiwa, G. Wallace, P. Bonoli, D. Brunner, I. Faust, A. Hubbard, B. LaBombard, and M. Porkolab, Plasma Phys. Controlled Fusion 55, 052001 (2013)

[12] G. M. Wallace, I. Faust, O. Meneghini, R. Parker, S. Shiraiwa, S. Baek, P. Bonoli, A. Hubbard, J. Hughes, B. LaBombard et al., Phys. Plasmas 19, 062505 (2012)

[13] S. Shiraiwa, G. Baek, P.T. Bonoli, I.C. Faust, A.E. Hubbard, O. Meneghini, R.R. Parker, G.M. Wallace, J.R. Wilson, R.W. Harvey, Nucl. Fusion 53, 113028 (2013)

[14] S. G. Baek, R. R. Parker, P. T. Bonoli, S. Shiraiwa, G. M. Wallace, B. LaBombard, I. C. Faust, M. Porkolab, D. G. Whyte, Nucl. Fusion 55, 043009 (2015)

[15] S. Shiraiwa, S. G. Baek, I. Faust, G. Wallace, P. Bonoli, O. Meneghini, R. Mumgaard, R. Parker, S. Scott, R. W. Harvey, B. J. Ding, M. H. Li, S. Y. Lin, and C. Yang, AIP Conf. Proc. 1689, 030016 (2015)

[16] A. Ekedahl, G. Granucci, J. Mailloux, Y. Baranov, S.K. Erents, E. Joffrin, X. Litaudon,A. Loarte, P.J. Lomas, D.C. McDonald, V. Petrzilka, K. Rantamäki, F.G. Rimini, C. Silva,M. Stamp, A.A. Tuccillo and JET EFDA Contributors, Nucl. Fusion 45, 351 (2005)

[17] R. R. Parker, G. M. Wallace, S. Shiraiwa, S.-G. Baek, I. C. Faust, 57th Annual meeting of the APS Division of Plasma Physics 60, BAPS.2015.DPP.CP12.2-(2015), http://meetings.aps.org/link/BAPS.2015.DPP.CP12.20

[18] M. Porkolab, Phys. Fluids 20, 2058 (1977)

[19] M. Preynas, M. Goniche, J. Hillairet, X. Litaudon, A. Ekedahl, and L. Colas, Nucl. Fusion 53, 013012 (2013)

[20] M. Madi, Y. Peysson, J. Decker, and K. Y. Kabalan, Plasma Phys. Contrl. Fusion 57, 125001 (2015)

[21] Y. Peysson, A. Ekedahl, E. Nilsson, M. Goniche, J.-F. Artaud, J. Hillairet, J. Decker, B. Ding, M. Li, P. Bonoli, S. Shiraiwa, M. Madi, "Advances in Modeling of Lower Hybrid Current Drive" , Accepted in Plasma Phys. Control. Fusion

[22] T. Shinya, S. G. Baek, G. M. Wallace, S. Shiraiwa, R. R. Parker, D. Brunner, B. LaBombard, and Y. Takase, 57th Annual meeting of the APS Division of Plasma Physics 60, BAPS.2015.DPP.CP12.22 (2015) http://meetings.aps.org/link/BAPS.2015.DPP.CP12.22

[23] S. G. Baek, G. M. Wallace, T. Shinya, S. Shiraiwa, R. R. Parker, Y. Takase and D. Brunner, AIP Conf. Proc. 1689, 080005 (2015)

[24] R. K. Fisher and R. W. Gould, *Phys. Rev. Lett.* **22**, 1093 (1969)

[25] T. Stix, Waves in plasmas (1992)

[26] D. Pozar, Microwave Engineering, John Wiley & Sons, Inc. (2005)

[27] A. Smirnov and R. Harvey, Bull. Am. Phys. Soc. 40, 1837 (1995)

[28] P. Bonoli and E. Ott, Phys. Fluids 25, 359 (1982)

[29] Y. Takase, M. Porkolab, J. Schuss, R. Watterson, C. Fiore, R. Slusher, and C. Surko, Phys. Fluids 28, 983 (1985)

[30] Y. Takase, R. L. Watterson, M. Porkolab, and C. L. Etme, Phy. Rev. Let. 53, 274 (1984)

[31] B. LaBombard, J. W. Hughes, N. Smick, A. Graf, K. Marr, R. McDermott, M. Reinke, M. Greenwald, B. Lipschultz, J. L. Terry, D. G. Whyte, S. J. Zweben, and Alcator C-Mod Team, Phys. Plasmas 15, 056106 (2008)